WASTES IV

solutions
treatments
opportunities

Editors:
Cândida Vilarinho, Fernando Castro & Margarida J. Quina

CRC Press
Taylor & Francis Group

WASTES: SOLUTIONS, TREATMENTS AND OPPORTUNITIES IV

WASTES: Solutions, Treatments and Opportunities IV contains selected papers presented at the 6th edition of the International Conference Wastes: Solutions, Treatments and Opportunities, that took place on 6-8 September 2023, in Coimbra, Portugal. The Wastes conference, which takes place biennially, is a prime forum for sharing innovations, technological developments and sustainable solutions for waste management and recycling sectors worldwide, with the participation of experts from academia and industry. The papers included in this book cover a wide range of topics, including:

– Management of waste streams
– Environmental, economic and social aspects in waste management
– Logistics, policies, regulatory constraints and markets in waste management
– Waste-to-energy technologies
– Life cycle assessment and carbon footprint
– Biological treatment techniques
– Waste treatment and valorization technologies
– Circular economy and industrial symbioses
– Smart technologies and digital tools in waste management
– Recycling of wastes and resources recovery
– Wastes refineries
– Food waste management and bioeconomy
– Plastic waste impacts, management strategies and solutions
– Wastes as critical raw materials resources

WASTES: Solutions, Treatments and Opportunities IV is aimed at academics and professionals involved in waste management and recycling sectors globally.

Wastes: Solutions, Treatments and Opportunities

Conference Selected Papers

ISSN 2640-9623

eISSN 2640-964X

Volume 4

Aims & Scope:

Wastes: Solutions, Treatments and Opportunities is an international conference that takes place every two years, organized by CVR - Centre for Waste Valorisation since 2011. The Wastes Conferences aim at bringing together academia and industry experts from the Waste Management and Recycling sectors, from around the world, offering state of the art knowledge and sharing experiences with all in attendance.

The Wastes Selected Papers Series presents the latest theoretical research and innovative technologies and techniques in the waste field, as well as tools and strategies to improve corporate environmental performance

SELECTED PAPERS FROM THE 6TH INTERNATIONAL CONFERENCE WASTES 2023,
6–8 SEPTEMBER 2023, COIMBRA, PORTUGAL

WASTES: Solutions, Treatments and Opportunities IV

Edited by

Cândida Vilarinho & Fernando Castro
University of Minho, Portugal

Margarida J Quina
University of Coimbra, Portugal

CRC Press
Taylor & Francis Group
Boca Raton London New York

CRC Press is an imprint of the
Taylor & Francis Group, an **informa** business
A BALKEMA BOOK

First published 2023
by CRC Press/Balkema
4 Park Square, Milton Park, Abingdon, Oxon, OX14 4RN

and by CRC Press/Balkema
2385 NW Executive Center Drive, Suite 320, Boca Raton FL 33431

CRC Press/Balkema is an imprint of the Taylor & Francis Group, an informa business

Typeset by Integra Software Services Pvt. Ltd., Pondicherry, India

British Library Cataloguing-in-Publication Data
A catalogue record for this book is available from the British Library

Library of Congress Cataloging-in-Publication Data

A catalog record has been requested for this book

ISBN: 978-1-032-38441-2 (hbk)
ISBN: 978-1-032-38442-9 (pbk)
ISBN: 978-1-003-34508-4 (ebk)
DOI: 10.1201/9781003345084

WASTES: Solutions, Treatments and Opportunities IV – Vilarinho, Castro & Quina (eds)

Table of contents

Purification of Green Hydrogen from Natural Gas Grids Using Zeolite 13X

L.F.A.S. Zafanelli, A. Henrique, E. Aly, J.A.C. Silva
Instituto Politécnico de Bragança, Bragança, Portugal

A.E. Rodrigues
Universidade do Porto, Porto, Portugal

ABSTRACT: Green hydrogen (GH) is a hot topic in the shift to clean energy, holding a promise to meet global energy demand while contributing to climate action goals. Its transportation can be done into Natural Gas (NG) grids, being necessary a separation technology to provide pure GH and NG to the end user. Accordingly, in this work, a series of breakthrough experiments evaluated the performance of binder-free zeolite 13X as a potential adsorbent to purify GH blended into NG grids. Single and multicomponent experiments were performed at 195, 231, and 273 K and pressure up to 1800 kPa. Noteworthy, the material enables a thermodynamic-based separation of these components due to its strong interaction with CH_4, resulting in selectivity values up to 17 at 195 K. The dual-site and standard Langmuir isotherm models fitted the adsorption equilibrium data, being the simulated multicomponent breakthrough curves suitably predicted by a homemade dynamic mathematical model.

1 INTRODUCTION

The GH produced by water electrolysis from renewable energy sources (e.g., wind, solar, hydroelectricity, and biomass) is free of carbon emissions, which can be a critical factor in decarbonizing heavy industry and achieving climate goals (IRENA 2018). Hydrogen is largely regarded as a potential future and cost-effective clean fuel due to its high calorimetric energy compared to other fuels, besides being sustainable and non-toxic. As the interest in GH grows, developing its distribution network is a hot topic in the scientific community. One alternative is to inject GH into the existing NG pipelines to avoid new infrastructure investments (IRENA 2019; van Renssen 2020; Melaina, Antonia, and Penev 2013). However, once the GH is injected into the NG grids, it must be extracted and purified to a high grade to use pure GH and NG separately when needed. For instance, GH should be purified by up to 99.97% to be converted into electricity by fuel cells (Liemberger et al. 2016). To date, pressure swing adsorption (PSA) processes are widely used for H_2 purification from steam methane reforming (SMR), which can achieve purities up to 99.9999 vol.%. The conventional PSA works very well for purifying H_2 from an SMR due to the high H_2 concentration in the feed (>70%). However, the allowed amount of H_2 that can be injected into the NG pipelines for distribution is limited to 20%, which challenges the GH/NG separation in the conventional PSA. In this view, to re-use PSA technologies as a solution, one would need an adsorbent material with a bigger CH_4 capacity than the currently available material.

2 MATERIALS & METHODS

2.1 *Materials*

The commercial binder-free beads of zeolite 13X evaluated in this work were provided by Chemiewerk Bad Köstritz GmbH (Germany). The beads consist of spherical particles with a diameter ranging from 1.6 to 2.5 mm, while the size of the zeolite crystals is around 2 μm. The material was manufactured through an advanced synthesis, in which the binder is itself transformed into zeolite matter during the hydrothermal reaction (Gleichmann, Unger, and Brandt 2016), overcoming the loss in adsorption capacity associated with the binder composite. The

structural and textural properties of the material were evaluated by nitrogen physisorption isotherms at 77 K and mercury intrusion porosimetry, both performed at the Laboratorio de Sólidos Porosos of the University of Málaga. The adsorbates H_2 (99.9999%), CH_4 (99.999%), He (99.9998%), and N_2 (99.999%) were supplied by Air Liquide.

2.2 *Cryogenic fixed bed breakthrough apparatus*

The adsorption equilibrium data of pure CH_4 and H_2 and its mixtures were evaluated in a chromatographic-based adsorption apparatus developed to measure fixed bed breakthrough curves. The experimental unit was specially designed to screen adsorbent materials at a wide range of temperatures, 77 to 333 K, and total pressure of up to 4000 kPa. Briefly, the cryogenic unit consists of three main sections: (i) gas preparation section, (ii) adsorption, and (iii) analytical section. In the gas preparation section, the flow rates of adsorbates (H_2 and CH_4), the inert helium (He), and the carrier gas nitrogen (N_2) are set up at the desired level through thermal mass flow controllers. A digital electronic back pressure regulator precisely establishes the system's total pressure. The adsorption section comprises a stainless-steel column (internal diameter 4.6 mm and length 100 mm, containing 970 mg of binder-free zeolite 13X) immersed in a Dewar flask cooling bath. The bath temperature is adjusted using a mixture of solvent and dry ice. In the last section, analytical, the outlet stream of the packed bed is directed to a gas chromatograph equipped with a capillary column (molar sieve 5A-plot: internal diameter 0.53 mm, length 15 m, and film thickness 50 μm) and a Thermal Conductivity Detector (TCD), which analyses its composition every 10 seconds with a 6-way sampling valve.

2.3 *Experimental procedure*

The single and multicomponent (mixture composition of CH_4/H_2: 80/20 vol.%) breakthrough experiments were performed covering the temperatures of 195, 233, and 273 K and total pressure up to 1800 kPa. Before the first experimental RUN, the binder-free beads of zeolite 13X were activated at a fixed temperature of 623 K for 12 h under pure He flow (5 mL/min) in a vacuum atmosphere. The activation step is essential to remove any pre-adsorbed moisture. The breakthrough experiments were conducted in order to ensure a gas residence time in the bed of around 40 seconds.

2.4 *Modelling and numerical simulation*

The equilibrium data obtained from the single component breakthrough curves were fitted with the dual-site Langmuir (CH_4) and Langmuir (H_2) isotherm models, and the data from the multicomponent experiments were modelled with the extended dual-site Langmuir model. Moreover, a general mathematical model has been developed to simulate and analyse the transient adsorption behaviour of H_2 and CH_4 of the binary breakthrough system. The numerical package comprises the fundamental partial differential equations (PDEs) distributed over time and space according to the material and energy conservation laws. In addition, it is augmented by a transport rate, the linear driving force model (Sircar and Hufton 2000), to account for the mass transfer between the fluid and solid phase. The collocation method was applied to discretise the spatial coordinate of the PDEs system (Villadsen and Michael 1978). The computation of the collocation points was determined by the position on the spatial coordinate using Jacobi polynomial, $P_N^{(\alpha,\beta)}(x)$, with $\alpha = \beta = 0$. Thus, the system of ordinary differential equations was solved using the ode15s integrator, a stiff ODE solver available in the MATLAB library (Shampine and Reichelt 1997), while the algebraic differential equations were solved by Gauss elimination.

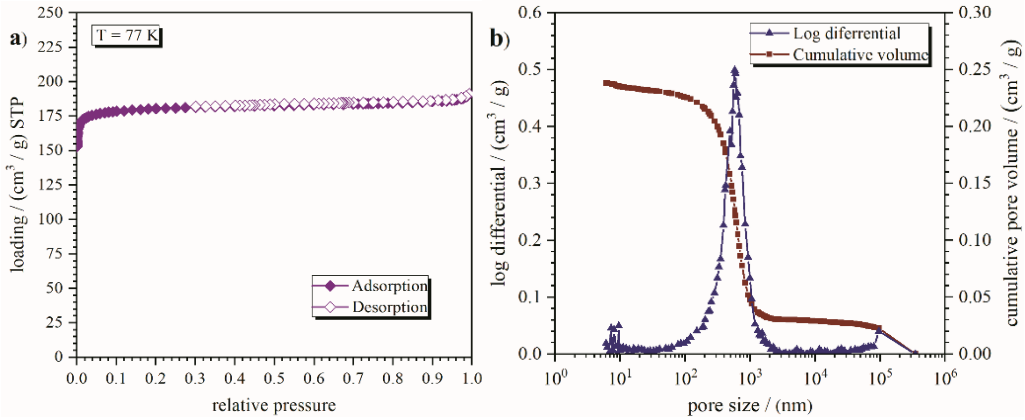

Figure 1. Characterisation of binder-free beads of zeolite 13X. a) N_2 adsorption and desorption isotherms at 77 K, and b) Macroscopic pore size and cumulative pore volume distribution.

2.5 *Objectives*

Based on Waste-to-energy technologies, this work aims to evaluate the performance of the commercial binder-free zeolite 13X as a potential adsorbent given the purification of GH blended into NG networks.

3 RESULTS AND DISCUSSIONS

3.1 *Adsorbent characterisation*

The N_2 adsorption and desorption isotherms at 77 K are shown in Figure 1a. As can be seen, they are of type I according to the updated International Union of Pure and Applied Chemistry (IUPAC) classification, being concave to the x-axis with the loadings approaching a constant value (horizontal plateau), which is a typical characteristic of microporous materials (Thommes et al. 2015). The steep uptake at a very low relative pressure (p/p0 between 10^{-5} to 10^{-2}) is related to enhanced gas-solid interactions in narrow pores, resulting in pore filling, in which the loading progressively increases to ≈185 cm^3/g. After filling the micropores, there are no regions where adsorption is significant, and the loading remains constant until $p/p_0 = 1$.

Table 1. Textural properties of the binder-free zeolite 13X.

N_2 adsorption data		
Langmuir surface area	m^2/g	792.50
External surface area	m^2/g	9.95
Micropore surface area	m^2/g	782.54
Micropore volume	cm^3/g	0.28
Total pore volume	cm^3/g	0.29
Hg porosimetry data		
Total intrusion volume	cm^3/g	0.24
Total pore area	m^2/g	4.61
Median pore diameter (volume)	nm	600.00
Median pore diameter (area)	nm	18.90
Average pore diameter (4V/A)	nm	206.80
Solid density	g/cm^3	1.73
Apparent density	g/cm^3	1.22
Porosity	%	29.16

Comparing the two branches of the isotherms, it is possible to assume that there is no hysteresis loop, indicating that the adsorption process is completely reversible. The results of the Hg intrusion porosimetry are given in Figure 1b. A unimodal macropore size distribution centred at 5.8 x

10^2 nm is observed and interpreted as originating from the intercrystalline pores between the individual zeolite 13X crystals. Additional information on the material's characterisation is summarised in Table 1.

3.2 *Single component adsorption of H_2 and CH_4 in binder-free zeolite 13X*

Figure 2 gathers the corresponding single component adsorption equilibrium isotherms for CH_4, and H_2 measured at (a) 195 K, (b) 231 K, and (c) 273 K. As it shows, the isotherms for CH_4 are marked type I according to IUPAC classification, while for H_2, they approach a linear shape. One can also note that the continuous lines in the figure demonstrate that the isotherm models conveniently describe the adsorption behaviour of CH_4 and H_2. The equilibrium data reveals a promising capacity of zeolite 13X for CH_4 capture, showing loadings significantly higher than for H_2 at the entire range of working conditions. For instance, at 195 K and 100 kPa, the loading obtained for CH_4 is 5.20 mol/kg in contrast with 0.17 mol/kg for H_2. This also means a selectivity ratio of around 30. These results indicate that binder-free zeolite 13X has excellent potential for the equilibrium separation of H_2 from H_2/CH_4 by PSA. The CH_4 is retained inside the column, whereas H_2 is recovered due to its weak interaction with the adsorbent material. Additionally, the isotherm for CH_4 became less steep as the temperature increased, meaning that this component can be easily desorbed, which is an added value for performing the regeneration step in the PSA process at room temperature.

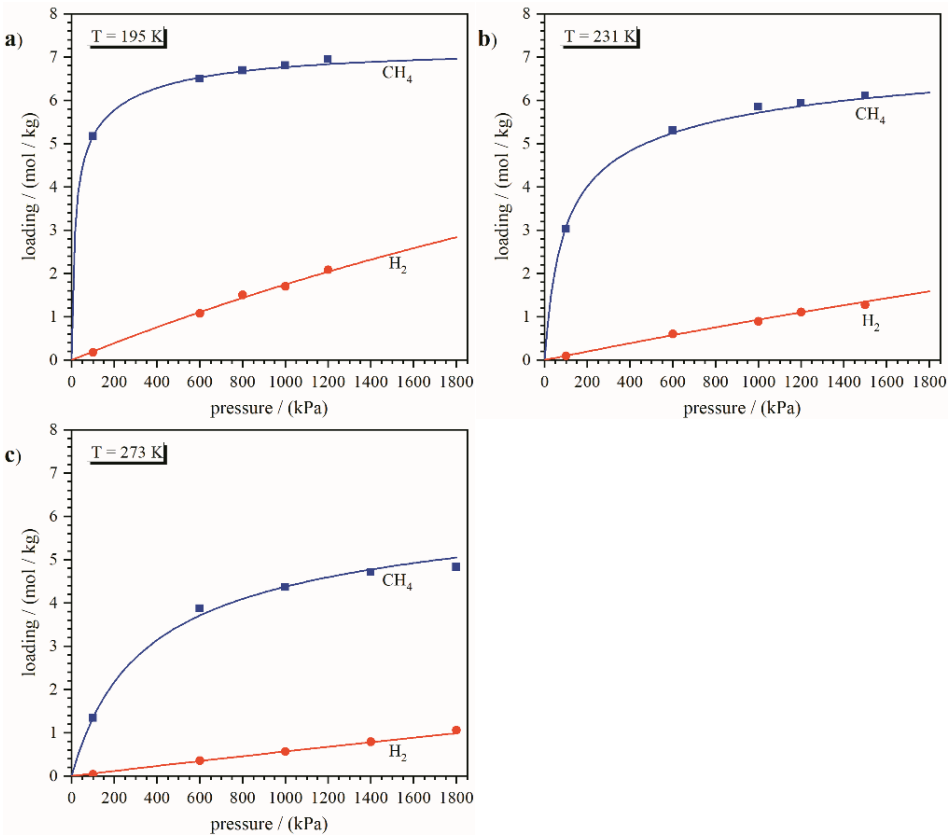

Figure 2. Single component adsorption equilibrium isotherms of CH_4 and H_2 in binder-free beads of zeolite 13X: a) 195 K, b) 231 K, and c) 273 K. The symbols stand for the experimental data, while the continuous lines represent the model predictions (CH_4: DLS and H_2: Langmuir).

Since we use binder-free beads, it is expected that the loading capacity increases, being of interest to compare our data with the zeolite 13X with the presence of binder (c.a. 15–25 %). Looking at the data measured by (Grande and Blom 2014), at 195 K and 100 kPa, the CH_4 loading in a conventional zeolite 13X is approximately 4.20 mol/kg, while the loading obtained in this work was 5.20 mol/kg. Therefore, the binder-free beads have a CH_4 adsorption capacity of 20% higher.

This result shows that it is possible to decrease the size of an adsorption column by 20% and reduce the CAPEX and OPEX in the industrial process.

3.3 *Multicomponent adsorption of H_2 and CH_4 in binder-free zeolite 13X*

The binary breakthrough curves of H_2/CH_4 (20/80 vol. %) are shown in Figure 3. The effect of the temperature is given: (a) 195, (b) 231, and (c) 273 K. These experiments confirmed the separation performance of binder-free zeolite 13X, resulting in a calculated selectivity $(q_{CH4}/y_{CH4})/(q_{H2}/y_{H2})$ up to 17.3 at 195 K (panel a). Moreover, the CH_4 loadings in a mixture with H_2 are very close to those observed in a single-component system, meaning that H_2 practically does not offer sorption competition with CH_4. As the temperature increases, the breakthrough time decreases from 9.2 (panel a) to 5.6 minutes (panel c) due to the exothermic nature of adsorption. The lines depicted in Figure 3 represent the simulation results, which suitably describe the experimental data. The linear mass transfer coefficients for CH_4 that were found to obtain the best fit of the binary breakthrough curves range from 0.0102 s^{-1} (195 K) to 0.0124 s^{-1} (273 K), while for H_2, a constant value of 1 s^{-1} was used.

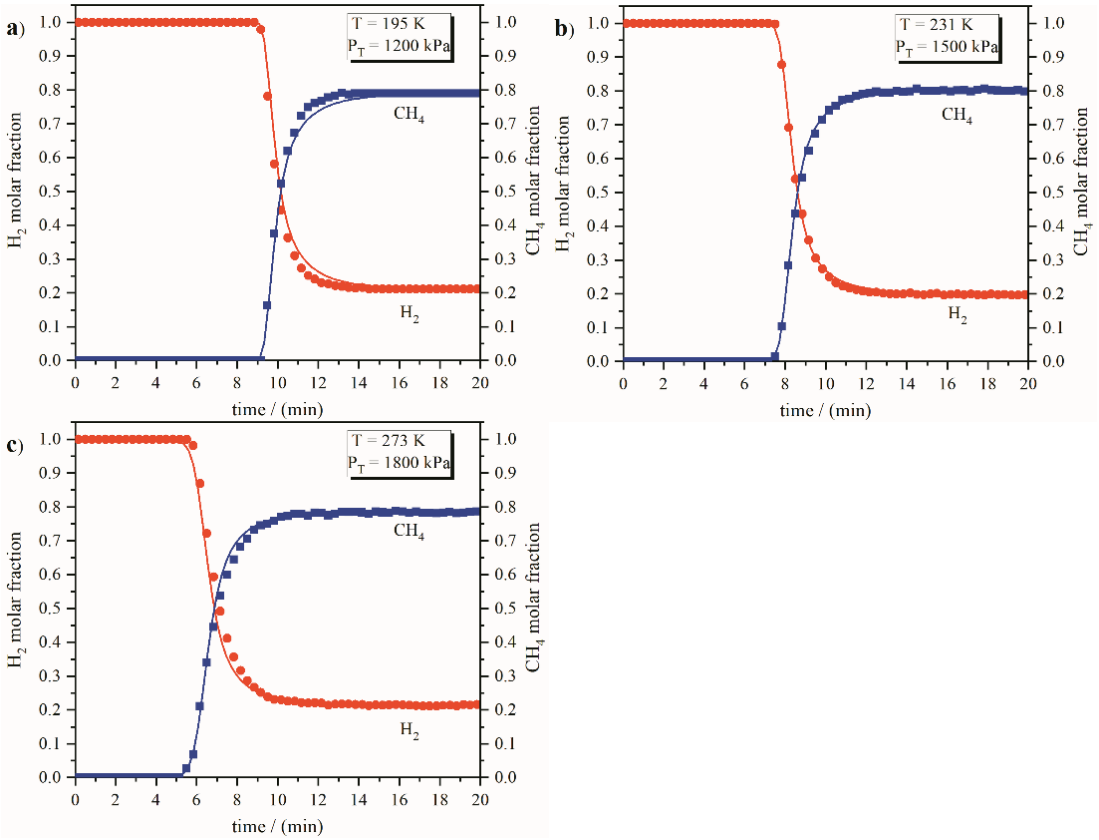

Figure 3. Breakthrough curves for a binary mixture of CH_4/H_2 (80/20 vol.%) in binder-free beads of zeolite 13X: a) 195 K, b) 231 K, and c) 273 K. The symbols stand for the experimental data, while the continuous lines represent the numerical simulations.

4 CONCLUSIONS

The binder-free zeolite 13X was considered a potential adsorbent to recover and purify GH blended into NG networks in this work. The single and multicomponent breakthrough experiments performed at cryogenic conditions demonstrated that the material has excellent performance for the equilibrium separation of H_2/CH_4, in which CH_4 is retained inside the column,

whereas H_2 is purely recovered at the outlet stream. The equilibrium data were suitably correlated with the dual-site (CH_4) and Langmuir (H_2) isotherm models. The fitted parameters were used in the numerical simulations, which adequately described the binary breakthrough curves, being the width of the mass-transfer zone well reproduced by accounting for low mass transfer resistances. The data collected in this work and the homemade simulator are now being used to study the cyclic operation (PSA) to purify H_2 from NG grids.

ACKNOWLEDGMENT

The authors are grateful to the Foundation for Science and Technology (FCT, Portugal) under project PTDC 2020 * 3599-PPCDTI * Engenharia dos Processos Químicos * project PTDC/EQU-EPQ/0467/ 2020. Also, through national funds FCT/MCTES (PIDDAC) to CIMO (UIDB/00690/2020 and UIDP/00690/2020), SusTEC (LA/P/0007/ 2021), ALiCE (LA/P/0045/2020), and LSRE-LCM (UIDB/50020/2020 and UIDP/50020/2020). Additionally, we thank national funding by FCT through the individual PhD research grant SFRH/BD/7925/2020 of Lucas F. A. S. Zafanelli. Moreover, the authors are grateful to Kristin Gleichmann and Chemiewerk Bad Koestritz GmbH for kindly providing the binder-free beads of zeolite 13X studied in this work.

REFERENCES

Gleichmann, Kristin, Baldur Unger, and Alfons Brandt. 2016. “Industrial Zeolite Molecular Sieves.” In *Intech*, i:13.

Grande, Carlos A., and Richard Blom. 2014. “Cryogenic Adsorption of Methane and Carbon Dioxide on Zeolites 4A and 13X.” *Energy & Fuels* 28 (10): 6688–93.

IRENA. 2018. *Hydrogen From Renewable Power: Technology Outlook for the Energy Transition*.

IRENA. 2019. *Hydrogen: A Renewable Energy Perspective*. 2nd ed. Tokyo: International Renewable Energy Agency, Abu Dhabi.

Liemberger, Werner, Markus Groß, Martin Miltner, Helga Prazak-Reisinger, and Michael Harasek. 2016. “Extraction of Green Hydrogen at Fuel Cell Quality from Mixtures with Natural Gas.” *Chemical Engineering Transactions* 52: 427–32.

Melaina, M W, O. Antonia, and M. Penev. 2013. “Blending Hydrogen into Natural Gas Pipeline Networks: A Review of Key Issues.” *National Renewable Energy Laboratory*. Vol. 303. Golden, CO (United States).

Renssen, Sonja van. 2020. “The Hydrogen Solution?” *Nature Climate Change* 10 (9): 799–801.

Shampine, L. F., and M. W. Reichelt. 1997. “The MATLAB ODE Suite.” *SIAM Journal on Scientific Computing* 18: 1–22.

Sircar, S, and J R Hufton. 2000. “Why Does the Linear Driving Force Model for Adsorption Kinetics Work ?,” 137–47.

Thommes, Matthias, Katsumi Kaneko, Alexander V. Neimark, James P. Olivier, Francisco Rodriguez-Reinoso, Jean Rouquerol, and Kenneth S.W. Sing. 2015. “Physisorption of Gases, with Special Reference to the Evaluation of Surface Area and Pore Size Distribution (IUPAC Technical Report).” *Pure and Applied Chemistry* 87 (9–10): 1051–69.

Villadsen, John, and L. Michelsen Michael. 1978. *Solution of Differential Equation Models by Polynomial Approximation*. *Englewood Cliffs, N. J., Prentice-Hall*. New Jersey.